



ISSN: 0067-2904
GIF: 0.851

Theoretical Study of New Derivative of Cefotaxime-Amic Acid as a Corrosion Inhibitor

Rehab M. Kubba^{1*}, Ahlam M. Al-Azzawi¹, Kafa K. Hammud²

¹ Department of Chemistry, College of Science, University of Baghdad, Baghdad, Iraq

² Ministry of Science and Technology, Baghdad, Iraq

Abstract

PM3 and DFT quantum mechanical calculations were employed to give further insight into the inhibition efficiency of the newly prepared cefotaxime amic acid derivative. The calculated physical properties and quantum chemical parameters correlated to the inhibition efficiency such as E_{HOMO} (highest occupied molecular orbital energy), E_{LUMO} (lowest unoccupied molecular orbital energy), the energy gap ($\Delta E_{(HOMO-LUMO)}$), hardness (η), softness (S), dipole moment (μ), electron affinity (EA), ionization potential (IE) and active site absorption....etc., all studied and discussed at equilibrium geometry in the gas phase and at its right symmetry (C_1). Experimentally the newly prepared cefotaxime derivative could be absorbed on carbon steel surface with good inhibition efficiency by offering electrons from rich hetero-atoms such as nitrogen and oxygen to unoccupied d-orbitals of Fe metal and forming antibonding orbital-feedback bonds.

Keywords: corrosion inhibitor, theoretical, PM3, DFT, Cefotaxime, amic acid derivative.

دراسة نظرية لمشتق جديد لحامض سيفوتاكسيم أميك كمثبط تآكل

رحاب ماجد كبة^{1*}، احلام معروف العزاوي¹، كفاء خلف حمود²

¹ كلية العلوم، قسم الكيمياء، جامعة بغداد، بغداد، العراق

² وزارة العلوم والتكنولوجيا، بغداد، العراق

الخلاصة

تضمن البحث استخدام حسابات ميكانيك الكم العائدة لطريقتي الحساب PM3 و DFT لاستكمال دراسة كفاءة تثبيط المشتق الجديد المحضر لحامض سيفوتاكسيم أميك. و تم حساب ومناقشة الخواص الفيزيائية ومعاملات ميكانيك الكم المرتبطة بدراسة كفاءة هذا المركب كمثبط تآكل مثل طاقة اعلى مدار مشغول بالالكترونات E_{HOMO} ، وطاقة اوطاً مدار غير مشغول بالالكترونات E_{LUMO} ، والفرق الطافي بينهما $\Delta E_{HOMO-LUMO}$ ، وتوزيع الكثافة الالكترونية والصلادة η و الليونة S وعزم ثنائي القطب μ والالفة الالكترونية EA و جهد التأين IE و مواقع الامتزاز الفعالة..... الخ، عند الشكل الهندسي التوازني وعند التماثل الصحيح للجزيئة (C_1). تجريبياً وجد امكانية امتزاز المركب على سطح الحديد الصلب كمثبط جيد للتآكل من خلال وهب الالكترونات من قبل الذرات الهجينة الغنية بالالكترونات مثل النتروجين والاكسجين الى مدار d غير المشغول بالالكترونات في عنصر الحديد مكونا اواصر استرجاعية.

*Email: Rehab_mmr_kb@yahoo.com

Introduction:

The β -lactam group as four-membered nitrogen-containing ring is one of the most important group of antibacterial agents used in clinical medicine esp. against gram-negative organisms and differ from penicillins by the heterocyclic ring system [1].

Cefotaxime is an antimicrobial agent commonly used for severe Salmonella infections, especially in children [2] and has an excellent activity against most strains of *S. pneumonia*, and high level resistance to penicillin [3].

Also, cefotaxime is considered as an excellent corrosion inhibitor (95.8%) in 1 M HCl solution by Shukla and Quarishi [4] as a result of the presence of free NH_2 group which gets strongly protonated in hydrochloric acid solution without considering its instability of in acidic media [5].

Corrosion by its simplest definition is the process of a metal returning to the material's thermodynamic state which is electrochemical reaction that follows the laws of thermodynamics and it is time and temperature dependent

Corrosion of metallic surfaces [6] can be controlled or reduced by the addition of chemical compounds to the corrodent. This form of corrosion control is called inhibition and the compounds added are known as corrosion inhibitors, which is one of the most common effective and economic methods to protect metals especially in acid medium [7].

The majority of the well-known inhibitors are organic compounds containing heteroatom, such as O, N, or S and that, at the same time, contain N and S in their structures are of particular importance since these provide an excellent inhibition compared with the compounds that contain only N or S [8]. The aim of this work is to study the corrosion efficiency parameters of the newly prepared cefotaxime pyromelliticdiamic acid as a good corrosion inhibitor with Parametric Methods PM3 and DFT using Gaussian 05 program.

Results and Discussion:

Cefotaxime introduced in reaction with pyromellitic dianhydride producing new pyromellitic acid containing different heterocycles (1). This reaction afforded characterized pyromellitic acid which linked to cefotaxime moiety with FTIR, ^1H NMR, and ^{13}C NMR spectroscopies as indicated in Figure-1 [9]. Values of the open circuit potential (OCP), the corrosion potential (E_{corr}), the corrosion current densities (I_{corr}), weight loss (wt loss), penetration loss, and protection efficiency (P%) for carbon steel at three different concentrations of cefotaxime-amic acid derivative and four different temperatures in 0.3N sulfuric acid were studied Table-1 [9].

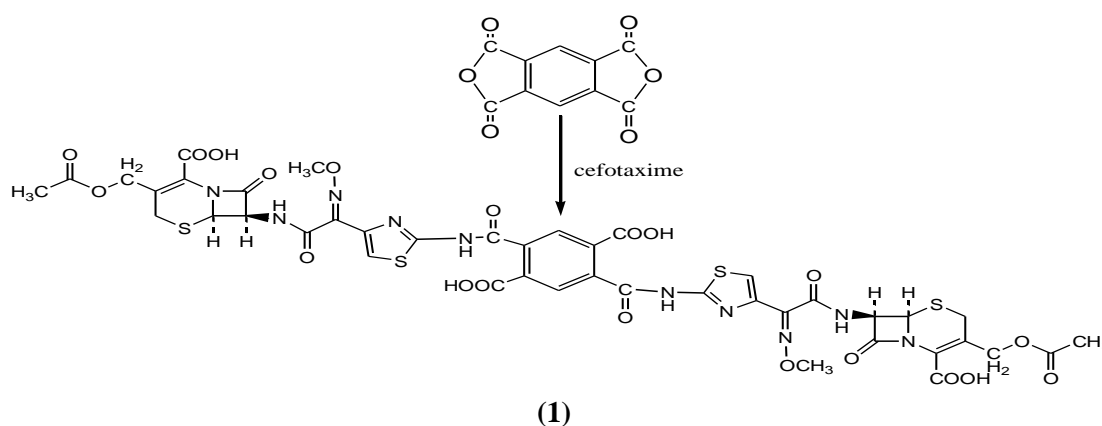


Figure 1- Chemical structure of 2,5-bis-{4-[(3-acetoxy-2-carboxy-8-oxo-5-thia-1-aza-bicyclo [4.2.0] oct-2-en-7-ylcarbamoyl)-methoxyimino-methyl]-thiazol-2-ylcarbamoyl}-terephthalic acid (pyromelliticdiamic acids).

Table 1- Experimentally values of the corrosion inhibition properties of cefotaxime-amic acid derivative on carbon steel at three different concentrations and four different temperatures in 0.3N sulfuric acid [9].

Condition	Conc.	Temp. K	OCP V	E _{corr} V	I _{corr} A/cm ² (x10 ⁻⁶)	Wt loss g.m ⁻² .d ⁻¹	Penetration mm. y	P%		
H ₂ SO ₄ with 1 mL DMSO	0.3 N	308	-0.510	-0.5092	939.28	235.00	10.90	-		
		318	-0.501	-0.4987	1320.00	330.00	15.30	-		
		328	-0.494	-0.4855	1310.00	328.00	15.20	-		
		338	-0.491	-0.4890	1730.00	432.00	20.10	-		
		308	-0.468	-0.4656	125.02	31.30	1.45	86.6808		
		318	-0.459	-0.4562	210.62	52.70	2.44	84.0303		
	50 ppm	328	-0.459	-0.4496	590.51	148.00	6.85	54.8780		
		338	-0.458	-0.4577	1120.00	280.00	13.00	35.1851		
		308	-0.454	-0.4424	307.46	76.90	3.57	67.2765		
		318	-0.454	-0.4436	639.05	160.00	7.42	51.5151		
		with 1 mL DMSO and 0.3 N H ₂ SO ₄	100 ppm	328	-0.453	-0.4523	896.45	224.00	10.40	31.7073
				338	-0.453	-0.4514	1330.00	331.00	15.40	23.3796
308	-0.475			-0.4641	385.12	96.30	4.47	59.0212		
150 ppm	318		-0.465	-0.4659	559.27	140.00	6.49	57.5757		
	328		-0.462	-0.4606	706.19	177.00	8.20	46.0365		
	338		-0.460	-0.4575	819.18	205.00	9.51	52.5462		

Inhibitor efficiency is higher for a compound which can donate electrons easily for the molecular site of adsorption and corresponds to high electron density at the presumed adsorption center in the molecular.

Most organic inhibitors are compounds with at least one polar function; the polar function is regarded as the reaction center for the establishment of the chemisorbed bond, whose strength is determined by the electron density of the atom acting as the reaction center [10].

A positive value of protection efficiency P% Table-1 indicates the inhibition of corrosion by the added inhibitors and it decreased with increasing in both its concentration and the applied temperature range. The variation in inhibitive efficiency with the concentration increasing of the acid may be attributed to the rate of evolution of hydrogen which may interfere with the absorption of the inhibitor on the metal surface.

From the experimental results, it is possible to get better performance with the newly prepared amic acid (1) as a corrosion inhibitor. The presence of different hetero-atoms with duplicate heterocycles in both sides of pyromelliticdiamic acids Figure-1.that may affect its action as corrosion inhibitors were investigated by theoretical calculations.

To correlate inhibition experimental data gained from electrochemical technique and the electronic–structural properties, quantum chemical calculations are extensively employed. Performing a quantum chemical study, a better understanding of the molecular structure- inhibitive effect relationship of pyromelliticdiamic acids may be concluded.

Quantum chemical study

The quantum chemical parameters for the optimized structure Figure-2 have been determined and analyzed in order to explain the interaction between the inhibitor molecules and the metal surface. According to DFT-Koopmans' theorem [11, 12], the HOMO energy is related to the ionization potential (IE) whereas the LUMO energy is linked to the electron affinity (EA), as follows:

$$\text{IE (Ionization potential)} = -E_{\text{HOMO}} \quad (1)$$

$$\text{EA (Electron affinity)} = -E_{\text{LUMO}} \quad (2)$$

Then, the electronegativity (χ), the chemical potential (μ) and the global hardness (η) were evaluated, based on the finite difference approximation, as linear combinations of the calculated IE and EA [13]:

$$\chi \text{ (Electronegativity)} = -\mu = (\text{IE} + \text{EA})/2 \quad (3)$$

$$\eta \text{ (Hardness)} = (\text{IE} - \text{EA})/2 \quad (4)$$

The global softness (S) is the inverse of the global hardness [14].

$$S \text{ (global softness)} = 1/\eta \quad (5)$$

Global electrophilicity index (ω) introduced by Parr [15], calculated using the electronegativity and chemical hardness parameters through the equation 6. A high value of electrophilicity describes a good electrophile while a small value of electrophilicity describes a good nucleophile [16].

$$\text{Global electrophilicity index } (\omega) = (-\chi)^2/2\eta \quad (6)$$

The fraction of transferred electrons (ΔN), evaluating the electronic flow in a reaction of two systems with different electronegativities, in particular case; a metallic surface and an inhibitor molecule was calculated according to Pearson theory [17] as:

$$\Delta N \text{ (Electron transferred)} = (\chi_{\text{Fe}} - \chi_{\text{inhib.}}) / [2(\eta_{\text{Fe}} + \eta_{\text{inhib.}})] \quad (7)$$

Where χ_{Fe} and χ_{inh} denote the absolute electronegativity of iron and inhibitor molecule respectively η_{Fe} and η_{inh} denote the absolute hardness of iron and the inhibitor molecule respectively.

In this study, we use the theoretical value of $\chi_{\text{Fe}} = 7.0\text{eV}$ and $\eta_{\text{Fe}} = 0.0\text{eV}$ for the computation of number of transferred electrons [18]. The difference in electronegativity drives the electron transfer, and the sum of the hardness parameters acts as a resistance [19]. The local selectivity of a corrosion inhibitor is best analyzed by means of condensed Fukui function.

Molecular geometry

With the Gauss View 03 implemented in Gaussian 03 package [20], its corresponding geometry was fully optimized using PM3 semiempirical method and Density Functional Theory (DFT) which was carried out using Becke's three-parameter functional and the correlation functional of Lee, Yang and Parr (B3LYP) at 6-311+G (d, p) level of theory [21, 22], and the vibrational calculations probe that their equilibrium structures correspond to the minima energy for Cefotaxime-amic acid derivative (absence of imaginary frequencies).

The final geometries and the computational results (bond lengths) of Cefotaxime-amic acid derivative corresponding to PM3 and DFT methods were given in Figure-2. Table-2, respectively. Figure-3 shows the label of the atoms of the studied inhibitor.

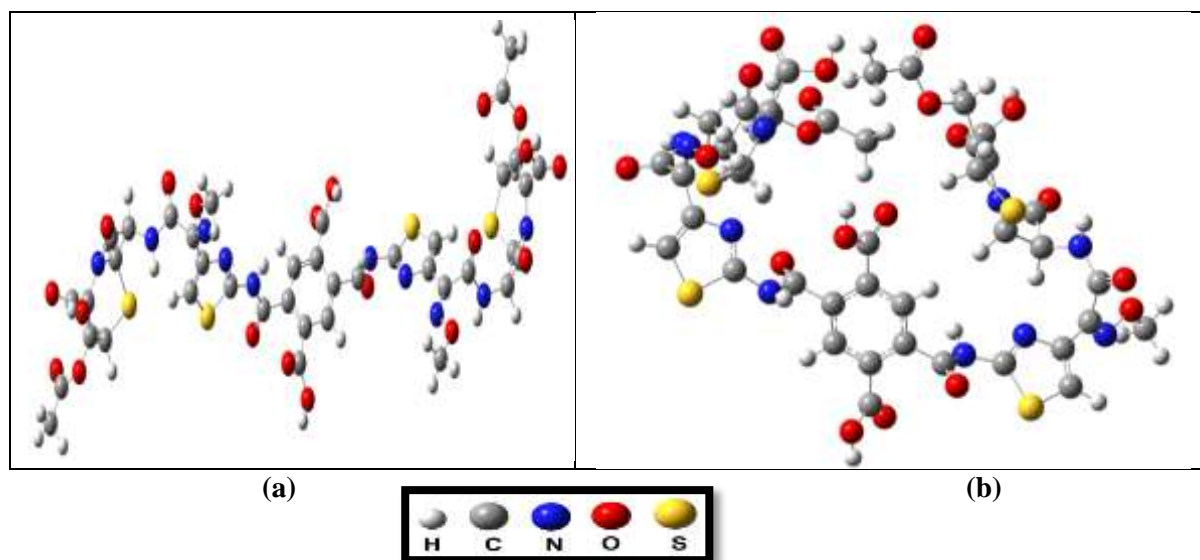


Figure 2- Equilibrium geometry of the inhibitor molecule calculated by (a) PM3 and (b) DFT methods.

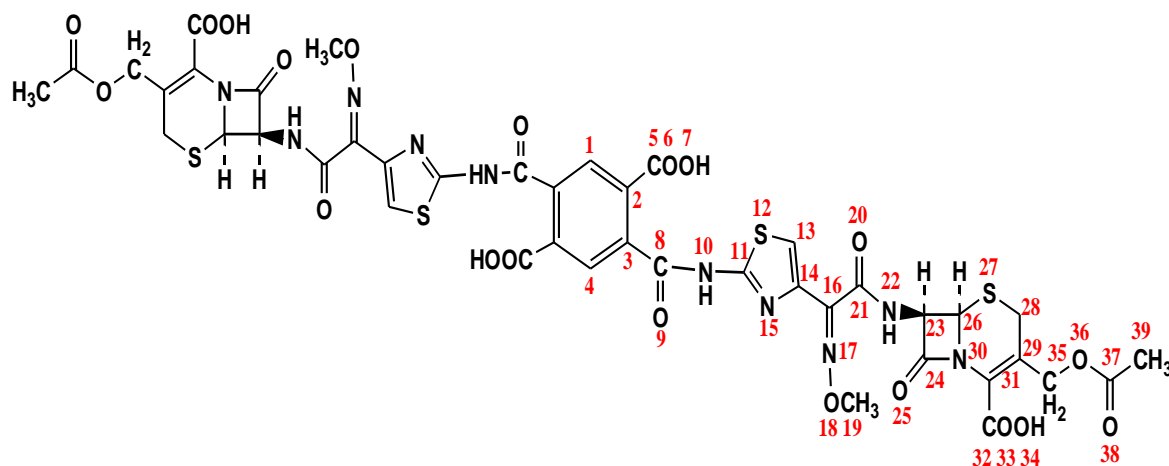


Figure 3- label of Cefotaxime–pyromelliticdiamic acid.

Table 2- Calculated geometric structure for Cefotaxime–pyromelliticdiamic acid molecule by using DFT B3LYP/6-311+G (d, p) method.

Description Bond	Bond length (Å)	Description Bond	Bond length (Å)	Description Bond	Bond length (Å)
C1-C2	1.39614	S12-C13	1.72431	C26-S27	1.82245
C2-C3	1.39474	C13-C14	1.37130	C26-N30	1.51213
C2-C5	1.48981	C14-N15	1.40743	S27-C28	1.82000
C3-C4	1.39720	C14-C16	1.47117	C28-C29	1.48848
C3-C8	1.50092	C16=N17	1.29680	C29=C31	1.35124
C5=O6	1.21549	N17-O18	1.40243	C29-C35	1.50698
C5-O7	1.35392	O18-C19	1.41150	C31-C32	1.49989
O7-H	0.95250	O20=C21	1.21825	C32-C34	1.35206
C8=O9	1.21601	C21-N22	1.42767	C32=O33	1.21533
C8-N10	1.42733	N22-C23	1.45994	C35-O36	1.42800
N10-C11	1.42252	C23-C24	1.55012	O36-C37	1.36693
C11-S12	1.76457	C23-C26	1.57147	C37-O38	1.21512
C11-N15	1.34220	C24=O25	1.19624	C37-O39	1.50040

The compound under investigation is not planar with C_1 point group with no symmetry operators for both PM3 and DFT calculations and was more distortion and higher dipole moment in DFT calculations due to the repulsion of its two ($\text{CH}_2\text{OCOCH}_3$) groups of terminal parts at which switching one over each other with a separate distance of (7.36886 Å) at the optimized calculated structure, Figure-2.

The computational results at the optimized geometrical structure of the studied inhibitor involve significant on the structural parameters such as bond angles Table-2. The largest values of the bond lengths were observed for **C26-S27** and **S27-C28** bonds which were longer than the **C11-S12** and **S12-C13** bonds. These differences can be explained by the less delocalization of electrons on **C26-S27-C28** than on **C11-S12-C13**. For this reason, it can be concluded that the adsorption on a metallic surface is clearly easy with **C26-S27** and **S27-C28** than with **C11-S12** and **S12-C13** bonds.

Global molecular reactivity

Frontier orbital theory is useful in predicting adsorption centers of the inhibitor molecules responsible of the interaction metallic surface/molecule [23]. The terms involving the Frontier Molecular Orbitals (FMO) could provide a dominative contribution, because of the inverse dependence of stabilization energy on orbital energy difference ($\Delta E = E_{\text{LUMO}} - E_{\text{HOMO}}$). The HOMO energy (E_{HOMO}) is often associated to the electron donating ability of the molecule, therefore, inhibitors with high values of E_{HOMO} have a tendency to donate electrons to appropriate acceptor with low empty molecular orbital energy. Conversely, the LUMO energy (E_{LUMO}) indicates the electron-accepting ability of the molecule, the lowest its value the higher the capability of accepting electrons. The gap energy between the frontier orbitals (ΔE) is another important factor in describing the molecular activity, so when the gap energy decreased, the inhibitor efficiency is improved [24].

The higher HOMO energy corresponds to the more reactive molecule in the reaction with electrophiles, while lower LUMO energy is essential for molecular reactions with nucleophiles.

The calculated quantum chemical parameters related to the inhibition efficiency of the studied molecule, such as the highest occupied molecular orbital (E_{HOMO}), energy of the lowest unoccupied molecular orbital (E_{LUMO}), energy gap ($\Delta E = E_{\text{LUMO}} - E_{\text{HOMO}}$), dipole moment (μ), the electronegativity (χ), the ionization potential (IP), the electron affinity (EA), the global hardness (η), and the fraction of electron transfer (ΔN) from the inhibitor molecules to iron, are collected in Table-2, Table-3, respectively, taking into consideration that the DFT calculation is the more accurate one.

HOMO and LUMO energies in the theoretical study used for prediction of inhibitor adsorption centers that interact with metal atom surface where E_{HOMO} values represent electron donation from the molecule (inhibitor) to the acceptor (metal surface) while E_{LUMO} values give a prior image of the acceptance of molecular electrons.[25,26]. Also, the HOMO-LUMO energy gap considered as an important factor in qualitative theoretical models for structural-conformation barriers. Indeed, the excellent corrosion inhibitors are usually the organic compounds which not only give electrons to the unoccupied orbital of the metal but also to accept free electrons from it [27].

The newly applied inhibitor with E_{HOMO} (-9.561, -2.857 eV), E_{LUMO} (-1.910, -6.767eV), $\Delta E_{(\text{HOMO-LUMO})}$ (7.651, 3.090eV) respectively which calculated according to PM3 and DFT methods. Table-3, showing that the inhibitor could be absorbed on carbon steel surface with good inhibition efficiency by offering electrons from rich hetero-atoms such as nitrogen, oxygen, and sulfur to unoccupied d-orbitals and forming antibonding orbital-feedback bonds [28].

The electronic properties at optimized molecular structure are given in Table-3, and Figure-4 with molecular orbital density illustrated large electric density of HOMO in thia-1-aza-bicyclo [4.2.0] oct-2-ene moiety in compound (1) whereas LUMO distributed in pyromellitic benzene ring for both the calculations even giving two different geometrical conformations.

The dipole moment (μ in Debye) is another very important electronic parameter that results from non uniform distribution of charges on the various atoms in the molecule. The high value of dipole moment increases the adsorption between a chemical compound and the metal surface. The dipole moment provides information on the polarity of the whole molecule. High dipole moment values are reported to facilitate adsorption (and therefore inhibition) by influencing the transport process through the adsorbed layer [29]. Several authors have stated that the inhibition efficiency increases with dipole moments values [30-31].

The dipole moments of the applied inhibitor are 9.787D and 11.072D, due to PM3 and DFT calculation methods respectively Table-3, which are higher than that of H_2O ($\mu = 1.88$ D) and higher than that of dipole moment for many good inhibitor compounds. The high dipole moment value of this compound probably indicates strong dipole-dipole interactions between the inhibitor and metallic surface [32].

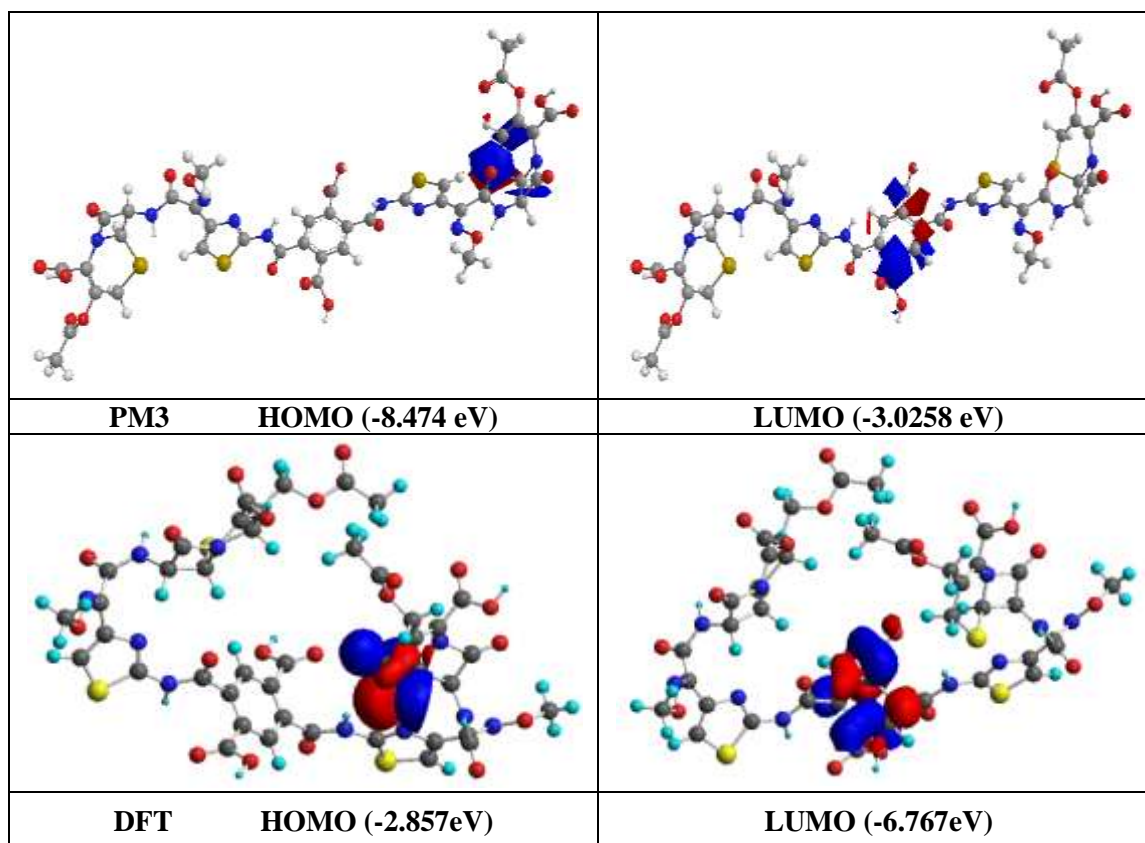
The fraction of electrons transferred (ΔN) from an inhibitor to mild steel surface was also calculated using a theoretical χ_{Fe} and η_{Fe} values for carbon steel of 7.0eV and 0.0eV respectively. The ΔN values are correlated to the inhibition efficiency resulting from electron donation. According to Lukovits et al. study [33], if $\Delta N < 3.6$, the inhibition efficiency increases with increasing electron-donating ability at the metal surface. The obtained values of ΔN reported in Table-3; show that the studied inhibitor has a higher value of ΔN (0.415, 0.559) Table-4 than ΔN of compounds mentioned in references [34-36] which were proved to have good efficiency corrosion. Therefore, the highest inhibition efficiency obtained experimentally for the calculated inhibitor can be explained by the tendency of a molecule to receive the electron by S atom in unoccupied orbital (3d). This ability to receive the electron from the metallic surface increases the inhibition efficiency.

Table 3- Some physical properties of the inhibitor molecule at the equilibrium geometries as calculated by using PM3 and DFT methods.

Inhib.	M. formula M. wt. (gm/mol)	E_{total} (eV)	ΔH_f (kcal/mol) (kJ/mol)	E_{HOMO} (eV)	E_{LUMO} (eV)	ΔE HOMO-LUMO (eV)	μ (Debye)
PM3	$\text{C}_{42}\text{H}_{36}\text{N}_{10}\text{O}_{20}\text{S}_4$ 1129.041	-----	-481.431 -2014.311	-9.561	-1.910	7.651	9.787
DFT		-143346.580	-----	-2.857	-6.767	3.090	11.4161

Table 4- Quantum chemical parameters for the inhibitor molecule as calculated by using PM3 and DFT method.

Inhib.	ꝀSym.	IE (eV)	EA (eV)	η (eV)	χ (eV)	S (eV)	(eV) ω	ΔN
PM3	C ₁	9.561	1.910	3.825	5.735	0.261	4.299	0.415
DFT	C ₁	6.767	2.857	1.955	4.812	0.511	5.922	0.559

**Figure 4-** The frontier molecule orbital density distributions of 2,5-bis-{4- [(3-acetoxy-2-carboxy-8-oxo-5-thia-1-aza-bicyclo [4.2.0] oct-2-en-7-ylcarbamoyl)- methoxyimino- methyl]-thiazol-2-ylcarbamoyl}-terephthalic acid compound as calculated by using PM3 and DFT method.**Active sites of the inhibitor molecule**

For the purpose of establishing the active sites of the inhibitor calculated molecule, three influencing factors: natural atomic charge, distribution of frontier molecular orbital and indices. According to classical chemical theory, all chemical interactions are either by electrostatic or orbital interactions. Electrical charges in the molecule were obviously the driving force of electrostatic interactions. It is proven that local electric densities or charges are important in many chemical reactions and physicochemical properties of compound [37]. Table-5 shows that the favored sites for electrophilic attack and the most reactive of the inhibitor molecule are C5, C8, C13, C24, C31, C32, C37 atoms of the thiazine ring and S12 heteroatom, the sites which can accept the electrons. Thus, for the nucleophilic attack the most reactive sites are C13, C28, C39 and O6, O7, O9, N10, N15, O18, O20, N30, O33, O34, O36, O38 heteroatom's. The negative charges centers could offer electrons to the Fe atoms to form a coordinate bond while the positive charge centers can accept electrons from 3d orbital of the Fe atom to form feedback bond, thus further strengthening the interaction of inhibitor and Fe surface.

The partial charges on the individual atoms in a molecule also indicate the reactive centers for a particular inhibitor. Atoms with the highest negative charge are considered to have an electron donor role when interacting with metal surfaces. The Mulliken atomic charges for the heteroatom's of the inhibitor molecule are reported in Table-5.

Based on the discussion above, it can be concluded that the inhibitor has many active centers for adsorption on carbon steel surface. Thus, the areas containing N, O and S atoms are the most favored sites for bonding to carbon steel surface through donating electrons. However, the S atom can give and receive the electron to and from metal, respectively. The last process reinforces the inhibitor molecule adsorption on a metallic surface.

Table 5- DFT Mulliken charges population analysis for the calculated inhibitor molecule.

Atom	Electronic charge						
C1	0.061	C11	0.158	C21	0.394	C31	0.318
C2	0.045	S12	0.349	N22	-0.364	C32	0.284
C3	-0.045	C13	-0.291	C23	0.126	O33	-0.319
C4	0.018	C14	0.197	C24	0.415	O34	-0.316
C5	0.263	N15	-0.359	O25	-0.281	C35	0.008
O6	-0.317	C16	0.009	C26	-0.137	O36	-0.337
O7	-0.315	N17	-0.115	S27	0.130	C37	0.311
C8	0.304	O18	-0.275	C28	-0.335	O38	-0.346
O9	-0.307	C19	-0.081	C29	-0.151	C39	-0.302
N10	-0.374	O20	-0.319	N30	-0.427		

Conclusion

The inhibition efficiency of carbon steel corrosion by Cefotaxime–pyrromelliticdiamic acid derivative has been investigated using quantum chemical calculations PM3 semiempirical method and (DFT/B3LYP/6-311) level of theory. The following conclusions were drawn from this study:

1. The geometrical parameters with both PM3 and DFT methods show that the inhibitor molecule is efficient for the corrosion inhibition. This result is in good agreement with experimental results studied previously.
2. A good correlation was found between the quantum chemical parameters calculated at equilibrium geometry by PM3 and DFT methods (E_{HOMO} , E_{LUMO} , gap energy (ΔE), dipole moment (μ) and the others with inhibition efficiency. This can be explained by the fact that the inhibitor compound can give and receive electrons from the metal, and these processes reinforce the adsorption of the inhibitor molecules on carbon steel surface.
3. The density distributions of the frontier molecular orbitals (HOMO and LUMO) show that Cefotaxime–pyrromelliticdiamic acid derivatives adsorb through the active centers nitrogen, oxygen, sulfur and π electrons of the benzothiazine ring.
4. The reactive site for electrophilic and nucleophilic attacks, determined from the DFT Mulliken charges population analysis for the calculated inhibitor molecule.

References:

1. Mandell, G. and Sande, M. **1990**. *Penicillins, Cephalosporin and other β -lactam antibiotics*, in: Goodman, A., Rall, T., Nies, A. and Taylor, P. Second Edition. Goodman and Gilman's *The pharmacological basis of therapeutics*, Pargamon Press, Elmsford, pp: 1065–1097.
2. Richards, D., Heel, R., Brogden, R., Speight, T. and Avery, G. **1984**. Ceftriaxone: A review of its antibacterial activity, pharmacological properties, and therapeutic use. *Drugs*, 27(6), pp: 469–527.
3. Klein, N. and Cunha, B. **1995**. Third-generation cephalosporins. *Med. Clin. North Am.*, 79(4), pp: 705–719.
4. Shukla, S. and Quraishi, M. **2009**. Cefotaxime sodium: a new and efficient corrosion inhibitor for mild steel in hydrochloric acid solution. *Corros. Sci.*, 51(5), pp:1007–1011.
5. Fabre, H., Hussam-Eddine, N. and Berge, G. **1984**. Degradation kinetics in aqueous solution of cefotaxime sodium, a third generation cephalosporin. *J. Pharm. Sci.*, 73, pp: 611–618.
6. Schweitzer, P. **2010**. *Fundamentals of Corrosion: Mechanisms, Causes, and Preventative Methods*. First Edition. CRC Press, Taylor and Francis Group, LLC, New York.
7. Hossain, S. and Almarshad, I. **2006**. Inhibiting effect of thiosemicarbazide on cold rolled carbon steel. *Corros. Eng. Sci. Technol.* 41(1), pp: 77-81.
8. Abdallah, M. Helal, E. and Fouda, A. **2006**. Aminopyrimidine derivatives as inhibitors for corrosion of 1018 carbon steel in nitric acid solution. *Corros. Sci.*, 48(7), pp: 1639-1654.
9. Al-Azzawi, A. M. and Hammud, K. K. **2014**. Inhibitive heteroamic acid behavior against 0.3N

- sulfuric acid corrosion of carbon steel. *J. Chem. Pharm. Res.*, 6(7), pp: 2808-2819.
10. Bentiss, F., Lebrini, M. and Lagrenée, M. **2005**. Thermodynamic characterization of metal dissolution and inhibitor adsorption processes in mild steel/2,5-bis(n-thienyl)-1,3,4-thiadiazoles/hydrochloric acid system. *Corrosion Science*, 47(12), pp: 2915–2931.
 11. Hehre, W., Radom, L., Schleyer, P. and Pople, J. **1986**. *AB INITIO Molecular Orbital Theory*. Second Edition. Wiley-Interscience. New York.
 12. Janak, J. **1978**. Proof that $\partial E/\partial n_i = \epsilon$ in density-functional theory. *Phys. Rev.*, B18, pp:7165–7168.
 13. Stowasser, R. and Hoffmann, R. **1999**. What do the Kohn-Sham orbitals and eigenvalues mean?. *J. Am. Chem. Soc.*, 121(14), pp: 3414–3420.
 14. Parr, R.G. and Pearson, R.G. **1983**. Absolute hardness: companion parameter to absolute electronegativity. *J. Am. Chem. Soc.*, 105, pp: 7512-7516.
 15. Parr, R., Donnelly, R., Levy, M., and Palke, W. **1978**. Electronegativity: the density functional approach. *J. Chem. Phys.*, 68, pp: 3801-3807.
 16. Pearson, R.G. **1988**. Absolute electronegativity and hardness: application to inorganic chemistry. *Inorganic Chemistry*, 27(4), pp: 734–740.
 17. Chermette, H. 1999. Chemical reactivity indexes in density functional theory. *J. Comput. Chem.*, 20, pp: 129-154.
 18. Ahamad, I., Prasad, R. and Quraishi, M. A. **2010**. Thermodynamic electrochemical and quantum chemical investigation of some Schiff bases as corrosion inhibitors for mild steel in hydrochloric acid solutions. *Corrosion Science*, 52 , pp: 933–942.
 19. Issa, R. M., Awad, M. K. and Atlam, F. M. **2008**. Quantum chemical studies on the inhibition of corrosion of copper surface by substituted uracils. *Appl. Surf. Sci.*, 255(5), pp: 2433–2441.
 20. Frisch, M.J., Trucks, G.W., Schlegel, H.B., Scuseria, G.E., Robb, M.A., Cheeseman, J.R., Montgomery, J.A., Jr., Vreven, T., Kudin, K.N., Burant, J.C., Millam, J.M., Iyengar, S.S., Tomasi, J., Barone, V., Mennucci, B., Cossi, M., Scalmani, G., Rega, N., Petersson, G.A., Nakatsuji, H., Hada, M., Ehara, M., Toyota, K., Fukuda, R., Hasegawa, J., Ishida, M., Nakajima, T., Honda, Y., Kitao, O., Nakai, H., Klene, M., Li, X., Knox, J.E., Hratchian, H.P., Cross, J.B., Bakken, V., Adamo, C., Jaramillo, J., Gomperts, R., Stratmann, R.E., Yazyev, O., Austin, A.J., Cammi, R., Pomelli, C., Ochterski, J.W., Ayala, P.Y., Morokuma, K., Voth, G.A., Salvador, P., Dannenberg, J.J., Zakrzewski, V.G., Dapprich, S., Daniels, A.D., Strain, M.C., Farkas, O., Malick, D.K., Rabuck, A. D., Raghavachari, K., Foresman, J. B., Ortiz, J. V., Cui, Q., Baboul, A. G., Clifford, S., Cioslowski, J., Stefanov, B.B., Liu, G., Liashenko, A., Piskorz, P., Komaromi, I., Martin, R.L., Fox, D.J., Keith, T. Al-Laham, M.A. Peng, C.Y. Nanayakkara, A. Challacombe, M. Gill, P.M. W. Johnson B. Chen, W., Wong, M.W., Gonzalez, C. and Pople, J.A. **2003**. *Gaussian 03*, Gaussian. Inc. Pittsburgh PA.
 21. Becke, A.D. **1993**. Density-functional thermochemistry. III. The role of exact exchange. *J. Chem. Phys.*, 98, pp: 5648-5652.
 22. Lee, C., Yang, W. and Parr, R.G **1988**. Development of the Colle-Salvetti correlation energy formula into a functional of the electron density. *Phys. Rev.*, B41, pp: 785-789.
 23. Fleming, I. **1976**. *Frontier Orbitals and Organic Chemical Reactions*. First Edition. John Wiley and Sons, New York.
 24. Fang, J. and Li, J. **2002**. Quantum chemistry study on the relationship between molecular structure and corrosion inhibition efficiency of amides. *J. Mol. Struct. (Theochem)*, 593(1-3): pp: 179–185.
 25. Musa, A., Mohamad, A., Kadhum, A., Takriff, M. and Ahmoda, W. **2012**. Quantum chemical studies on corrosion inhibition for series of thio compounds on mild steel in hydrochloric acid. *J. Indus. Eng. Chem.*, 18(1), pp: 551–555.
 26. Khaled, F. **2010**. Experimental, density function theory calculations and molecular dynamics simulations to investigate the adsorption of some thiourea derivatives on iron surface in nitric acid solutions. *Appl. Surf. Sci.*, 256, pp: 6753–6763.
 27. Khalil, N. **2003**. Quantum chemical approach of corrosion inhibition. *Electrochim. Acta.*, 48(20), pp: 2635–2640.
 28. Wang, H., Wang, X., Wang, H., Wang L. and Liu, A. **2007**. DFT study of new bipyrazole derivatives and their potential activity as corrosion inhibitors. *Journal of Molecular Modeling*, 13(1), pp: 147-153.
 29. a-Obot, B., Obi-Egbedi, N. O. and Umoren S. A. **2009**. Adsorption characteristics and corrosion inhibitive properties of clotrimazole for aluminium corrosion in hydrochloric acid. *Int. J.*

- Electrochem. Sci.*, 4, pp: 863-877.
30. Popova, A., Christov, M. and Deligeorgiev, T. **2003**. Influence of the molecular structure on the inhibitor properties of benzimidazole derivatives on mild steel corrosion in 1 M hydrochloric acid, *Corros.*, 59(9), pp: 756–764.
 31. Sahin, M., Gece, G., Karci, F. and Bilgic, S. **2008**. Experimental and theoretical study of the effect of some heterocyclic compounds on the corrosion of low carbon steel in 3.5% NaCl medium, *J. Appl. Electrochem.*, 38(6), pp: 809–815.
 32. Quraishi, M. and Sardar, R. **2003**. Hector bases—a new class of heterocyclic corrosion inhibitors for mild steel in acid solutions. *J. Appl. Electrochem.*, 33(12), pp: 1163–1168.
 33. Lukovits, I., Kalman, E. and Zucchi, F. **2001**. Corrosion inhibitors—correlation between electronic structure and efficiency. *Corros.*, 57(1), pp: 3–8.
 34. Kubba, R.M. and Abood, F.K. **2015**. DFT, PM3, AM1, and MINDO/3 quantum mechanical calculations for some INHC Cs symmetry Schiff bases as corrosion inhibitors for mild steel. *Iraqi Journal of Science*, 56(1C), pp: 602-621.
 35. Kubba, R.M. and Abood, F.K., **2015**, Quantum chemical investigation of some schiff bases as corrosion inhibitors for mild steel in hydrochloric acid solutions., *Iraqi Journal of Science*. 56(2B), pp: 1241-1257.
 36. Obi-Egbedi, N.O., Obot, I.B., El-Khaiary, M.I., Umoren, S.A. and Ebenso, E.E. **2011**. Computational simulation and statistical analysis on the relationship between corrosion inhibition efficiency and molecular structure of some phenanthroline derivatives on mild steel surface. *Int. J. Electro Chem. Sci.*, 6(11), pp: 5649-5675.
 37. Sandip, K.R., Islam, N. and Dulal, C.G. **2011**. Modeling of the chemico-physical process of protonation of molecules entailing some quantum chemical descriptors. *J. Quantum Information Science*, 1, pp: 87-95.